Wave Digital Implementation of Robust First-Order Differential Microphone Arrays

Alberto Bernardini, *Student Member, IEEE*, Fabio Antonacci, *Member, IEEE*,
Augusto Sarti, *Senior Member, IEEE*

Abstract—In this letter, a novel time-domain implementation of robust first-order Differential Microphone Arrays (DMAs), based on Wave Digital Filters, is presented. The proposed beamforming method is extremely efficient, as it requires at most two multipliers and one delay for each filter, where the necessary number of filters equals the number of physical microphones of the array, and it avoids the use of fractional delays. The update of the coefficients of the filters, required for reshaping the beampattern, has a significantly lower computational cost with respect to the time-domain methods presented in the literature. This makes the proposed method suitable for real-time DMA applications with time-varying beampatterns.

Index Terms—Differential Microphone Arrays, Wave Digital Filters, Beamforming

I. INTRODUCTION

DIFFERENTIAL beamforming methods [1]–[4] applied to small-size microphone arrays, e.g. arrays of MEMS microphones [5], are attractive for spatial filtering of broadband audio signals, such as speech signals, e.g. in hands-free [6] and automotive [7] communication systems, as they exhibit almost frequency invariant beampatterns [1]. Earliest implementations of First Order DMAs (FODMAs) involved only a pair of physical omnidirectional microphones, whose fractionally delayed output signals were subtracted and then low pass filtered [8]–[10]. Robust DMAs [11], [12] are a generalization of such implementations, as they include an arbitrary number $M \geq 2$ of physical microphones in the acoustic model and are characterized by better SNR w.r.t. traditional DMAs. Robust DMAs theorized in [11] are based on the Taylor series approximation of the exponentials in the steering vector, while those in [12] are based on the Jacobi-Anger expansion of the same exponentials. Robust DMAs in [11] can be implemented more efficiently than the ones in [12], as the latter require the tabulation and/or approximation of Bessel functions. However, the models presented in [12] are more accurate when distances between microphones pairs are increased. The majority of the recently proposed DMA models are provided in the frequency domain [1], [11], [12], ready to be implemented using Short-Time Fourier Transform (STFT) filtering. However, as outlined in [13], time-domain implementations of DMA would be highly desirable, especially in

applications in which small delays are required, such as real-time communication systems. Moreover, filtering in the time domain is more efficient than using STFT, when the number of filter taps is sufficiently small. Finally, time-domain filtering does not suffer from undesired edge effects typical of methods based on the STFT. For these reasons, in [13] a closed-form solution for broadband time-domain FODMAs for any given number of sensors $M \geq 2$ is provided. A drawback of the approach in [13] is that the derivation of filter coefficients implies the inversion of a multi-dimensional linear system, which is computationally costly.

In the light of the above considerations, in this letter, we will propose a novel time-domain FODMA implementation. Firstly, the frequency-domain FODMA model presented in [11] is resumed and an electrical equivalent representation of it, never appeared in the literature, is presented. In particular, the FODMA will be represented with M separated simple electric circuits, where M is the number of physical microphones. Starting from the derived reference circuits, we will show how to design the corresponding Wave Digital Filters (WDFs) [14]–[16]. Each WDF will be characterized by an explicit input-output function in closed form, where the input signal will be the signal sensed by the corresponding physical microphone. The global output of the beamformer will be the sum of the output signals of the M WDFs. We will show that the proposed time-domain filtering method based on WDFs requires less computational operations than the one presented in [13] and no fractional delays to be designed. Moreover, the computational cost for updating the filter coefficients is dramatically reduced w.r.t. [13]. This makes the proposed method suitable for DMAs in which the beampattern is required to change over time; e.g. when the directivity of the beampattern needs to be frequently regulated on the fly or when the position of its nulls needs to be adjusted for attenuating a moving interference. We will also show that, at speech frequencies, the White Noise Gain and the Directivity Factor of the derived FODMA based on WDFs are almost coincident to the same SNR measures in the continuous case, even using relatively low audio sampling rates (e.g. $F_s = 16$ kHz).

II. CIRCUIT REPRESENTATION OF ROBUST FODMAS

A. Background: Signal Model and Beampattern Definition

Let us consider a linear microphone array with M uniformly spaced omnidirectional sensors [11]; the distance in meters between consecutive sensors is δ. Let us then consider the 2D plane that contains all the sensors and a sound source

A. Bernardini, F. Antonacci and A. Sarti are with the Dipartimento di Elettronica, Informazione e Bioingegneria, Politecnico di Milano, Piazza Leonardo Da Vinci 32, 20133 Milano, Italy (e-mail: [alberto.bernardini,fabio.antonacci,augusto.sarti]@polimi.it).

in far field. The source is assumed to emit a plane wave, which propagates at the speed of sound, e.g. $c = 340$ m/s, and impinges the microphone array. The wave front of the plane wave forms an angle θ with the array line; θ is the direction of arrival of the source. According to [11], the steering vector is defined as

$$\mathbf{d}(\omega, \theta) = \left[1, e^{-j\omega\tau_0\cos\theta}, \ldots, e^{-j(M-1)\omega\tau_0\cos\theta}\right]^T$$

where T denotes transposition, j is the imaginary unit, $\omega = 2\pi f$ is the analog angular frequency, $f > 0$ is the temporal frequency, and $\tau_0 = \delta/c$ is the delay between two successive sensors when the source is at the endfire direction $\theta = 0$. The vector of the signals sensed by the M microphones is

$$\mathbf{y}(\omega) = [Y_1(\omega), \ldots, Y_M(\omega)]^T = \mathbf{d}(\omega, 0)X(\omega) + \mathbf{w}(\omega)$$

where $X(\omega)$ is the desired source signal, $\mathbf{w}(\omega)$ is the additive noise signal vector of dimension M. The mth microphone signal with $1 \leq m \leq M$ is filtered by a properly designed filter $H_m(\omega)$. All the filters are collected in the vector $\mathbf{h}(\omega) = [H_1(\omega), \ldots, H_M(\omega)]^T$. Then, according to [11], the output signal of the robust differential beamformer is defined as

$$Z_0(\omega) = \sum_{m=1}^{M} H_m^*(\omega) Y_m(\omega) = \mathbf{h}^H(\omega)\mathbf{y}(\omega) \qquad (1)$$

where the superscripts $*$ and H denote the complex conjugation operator and the hermitian operator, respectively. The frequency-independent beampattern of a FODMA is

$$\mathcal{B}(\theta) = 1 - q + q\cos\theta \qquad (2)$$

where $0 \leq q \leq 1$ determines the beam shape [10]. As shown in [11], the FODMA filters $H_m(\omega)$ are given by

$$H_1(\omega) = \frac{-3q}{(2M-1)j\omega\tau_0} + 1 - q \quad , \qquad (3)$$

$$H_k(\omega) = \frac{6(k-1)}{(2M^3 - 3M^2 + M)j\omega\tau_0}, \, k = 2, 3, \ldots, M. \quad (4)$$

B. Electrical Equivalents of Robust FODMA Filters

In this Subsection we show how robust FODMA described in [11] can be equivalently represented with a bank of M circuits, whose suitably chosen output signals are summed for deriving the global beamformer output signal. Each circuit is derived considering the mth contribute of the sum (1) as a voltage signal, so that the conjugate filters $H_m^*(\omega)$ are interpreted as electric impedances and the signals $Y_m(\omega)$ are assumed to be generated by ideal current sources. Therefore, formula (1) can be formally rewritten as $Z_0(\omega) = \sum_{m=1}^{M} V_{0m}(\omega)$ where $V_{0m}(\omega) = H_m^*(\omega) Y_m(\omega)$ are the aforementioned voltage signals. It follows that, according to the above electrical interpretation of the results presented in [11], $H_1^*(\omega)$ can be represented as the series of a capacitor with capacitance C_1 and a resistor with resistance R_1. Formally,

$$H_1^*(\omega) = \frac{1}{j\omega C_1} + R_1 \qquad (5)$$

where

$$C_1 = \frac{(2M-1)\tau_0}{3q} \quad , \qquad R_1 = 1 - q \quad .$$

(a) 1st circuit   (b) kth circuit
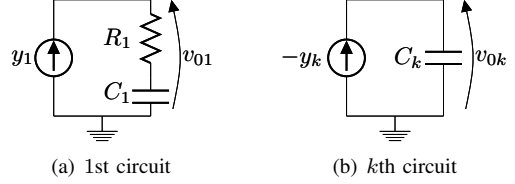
Fig. 1. Equivalent circuits.

Similarly, $H_k^*(\omega)$ can be represented as a capacitor in the form

$$H_k^*(\omega) = -\frac{1}{j\omega C_k} \qquad (6)$$

where $k = 2, \ldots, M$ and the capacitance C_k is expressed as

$$C_k = \frac{(2M^3 - 3M^2 + M)\tau_0}{6q(k-1)} \quad .$$

Fig. 1 shows the resulting equivalent circuits; the circuit in Fig. 1(a) refers to sensor 1, while the circuit in Fig. 1(b) refers to sensor k, being $2 \leq k \leq M$. The signals y_1, v_{01}, y_k and v_{0k} written in lower case are the time-domain versions of the frequency-domain signals Y_1, V_{01}, Y_k and V_{0k}, respectively.

III. WAVE DIGITAL FODMA MODEL

Disposing of electrical equivalents of robust FODMAs makes them particularly suitable to be implemented using WDFs. The reference circuits in Fig. 1 are stable; therefore, as WDFs are known to preserve the energetic properties of the reference analog circuits [14], their WDF realization will be stable as well and it will exhibit low sensitivity to parameter variation [17]. In this Section, after a brief recap of basic WDF theory, we will derive an efficient Wave Digital implementation of FODMAs with at most two multipliers and one delay per microphone.

A. Background on WDFs

WDFs are designed starting from a port-wise consideration of a *reference analog circuit*, which is then discretized and implemented in the digital domain using input-output blocks. Circuit elements and the interconnection topology are modeled using separated blocks which are then connected in a port-wise fashion. Each pair of Kirchhoff port variables, i.e. port current i and port voltage v, of the reference circuit is mapped to a pair of *wave signals*, i.e. incident wave a and reflected wave b, according to the following linear transformation

$$a = v + R_0 i \qquad\qquad b = v - R_0 i \qquad (7)$$

where R_0 is a free parameter called *port resistance*. Free parameters are exploited for turning circuit networks into computable input-output digital structures. This is accomplished by setting the port resistances in such a way that instantaneous dependencies between wave signals are eliminated. This process is called *adaptation* in WDF theory. For the details on how adaptation is performed the reader is referred to [14]. Here follows a brief review of the wave mappings for the circuit elements and topological junctions used in the WDF implementation in Fig. 2 relative to the circuits in Fig. 1.

(a) 1st WDF   (b) kth WDF
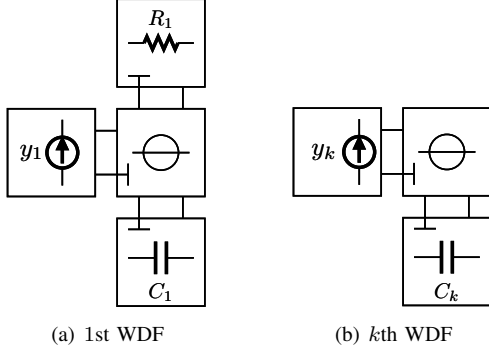
Fig. 2. WDF representation of equivalent circuits in Fig. 1; Fig. 2(a) refers to Fig. 1(a), while Fig. 2(b) refers to Fig. 1(b).

1) Resistor: Kirchhoff port variables of a linear resistor with resistance R are related by $v = Ri$, and the relative wave mapping is $b = [(R - R_0) / (R + R_0)] a$. The resistor can be adapted by setting $R_0 = R$; in this case the wave mapping becomes $b = 0$ and the instantaneous dependence between the wave signals a and b is eliminated.

2) Capacitor: The constitutive equation of a capacitor with capacitance C in the Laplace domain is $V(s) = I(s) / (sC)$, where $s = j\omega$ is the complex frequency. The continuous-time signals are discretized performing the bilinear transform and the wave mapping in the discrete-time domain is derived. Imposing the adaptation condition $R_0 = 1/(2F_sC)$, the simple explicit time-domain wave mapping $b[n] = a[n-1]$ relative to the nth sampling step is obtained.

3) Ideal Current Source: The wave mapping of an ideal current source I_G characterized by the constraint $i = I_G$ is $b = a - 2R_0 I_G$. Ideal sources cannot be adapted in the wave domain; therefore, we need to adapt the corresponding port of the topological junction to which they are connected.

4) Series Adaptors: The multidimensional scattering relation of a N-port series junction is $\mathbf{a} = \mathbf{S}_N \mathbf{b} = (\mathbf{I} - \alpha_N \mathbf{1}^T) \mathbf{b}$, where $\mathbf{b} = [b_1, \ldots, b_N]^T$ is the vector of wave signals reflected from the elements and incident to the junction, $\mathbf{a} = [a_1, \ldots, a_N]^T$ is the vector of wave signals incident to the elements and reflected from the junction, $\mathbf{S}_N$ is the scattering matrix, $\alpha_N = 2/\left(\sum_{i=1}^{N} R_{0i}\right) [R_{01}, \ldots, R_{0N}]^T$, R_{0i} is the ith port resistance, $\mathbf{I}$ is the $N \times N$ identity matrix and $\mathbf{1}$ is a column vector of N ones. A port of the junction, e.g. port 1, can be adapted if we set $R_{01} = \sum_{i=2}^{N} R_{0i}$. The resulting scattering matrices in the 2-port and 3-port cases are

$$\mathbf{S}_2 = -\begin{bmatrix} 0 & 1 \\ 1 & 0 \end{bmatrix}, \mathbf{S}_3 = \frac{-1}{R_{02} + R_{03}} \begin{bmatrix} 0 & R_{02} + R_{03} & R_{02} + R_{03} \\ R_{02} & -R_{03} & R_{02} \\ R_{03} & R_{03} & -R_{02} \end{bmatrix}.$$

B. Proposed Robust FODMA Implementation

A WDF implementation of the circuits in Fig. 1 can be easily obtained using the equations provided in the previous subsection and the implementation schemes in Fig. 2. As according to the considerations in Section II-B, only v_{0m} with $1 \le m \le M$ is needed as output signal of the mth circuit the time-domain implementation of each filter of the beamformer

TABLE I
MULTIPLICATIONS (MUL), ADDITIONS (ADD) AND PAST SAMPLES (MEM) REQUIRED FOR UPDATING THE FILTER COEFFICIENTS AND FILTERING

	WDF Model		Model in [13]	
	Update	Filtering	Update	Filtering
mul	$2M$	$2M$	$\approx 3(L_h M)^3$	$L_h M$
add	2	$3M - 1$	$\approx 3(L_h M)^3$	$L_h M - 1$
mem	0	M	0	$L_h M - M$

can be simplified. In particular for $m = 1$, at the sampling step n we can write

$$\begin{bmatrix} a_{C1}[n] \\ v_{01}[n] \end{bmatrix} = \begin{bmatrix} 1 & \eta_1 \\ 1 & \gamma_1 \end{bmatrix} \begin{bmatrix} a_{C1}[n-1] \\ y_1[n] \end{bmatrix} \tag{8}$$

where $\eta_1 = T/C_1$, $\gamma_1 = \eta_1/2 + R_{C1}$ and a_{C1} is the wave signal incident to the capacitor element C_1. Similarly for $m = k$ with $2 \le k \le M$, we can write

$$\begin{bmatrix} a_{Ck}[n] \\ v_{0k}[n] \end{bmatrix} = \begin{bmatrix} 1 & \eta_k \\ -1 & \gamma_k \end{bmatrix} \begin{bmatrix} a_{Ck}[n-1] \\ y_k[n] \end{bmatrix} \tag{9}$$

where $\eta_k = T/C_k$, $\gamma_k = -\eta_k/2$ and a_{Ck} is the wave signal incident to the capacitor element C_k. The time-domain global output signal of the beamformer is simply computed as

$$z_0[n] = \sum_{m=1}^{M} v_{0m}[n] . \tag{10}$$

In accordance to equations (8), (9) and (10), the time-domain signal flow in Fig. 3 shows how to realize the proposed FODMA implementation.

C. Computational Cost Analysis

The cost, in terms of number of computational operations, and the number of past samples, required by the proposed WDF model and the model in [13], for updating the filter coefficients and filtering, is reported in Table I. As far as the update is concerned, the WDF approach is far more efficient, as it requires only $2M$ multiplications and 2 additions. Conversely, the method in [13] involves populating a $2(2L_D + L_{fd} + L_h) \times ML_h$ matrix (where $L_D = \lceil (M-1)\tau_0 F_s \rceil$, L_{fd} is the length of the causal fractional delay filters and L_h is the length of the M temporal filters) and the computation of its pseudo-inverse. It follows that the number of multiplications is a function of M, L_h, L_D and L_{fd} which, for practical values of such parameters, is roughly in the order of $3(L_h M)^3$. Similar considerations hold for additions. As outlined in Table I, also filtering is more efficient if the proposed WDF approach is adopted, even though the efficiency gain is less pronounced than in the update phase.

IV. SIGNAL-TO-NOISE RATIO (SNR) ANALYSIS

SNR in DMAs is called White Noise Gain (WNG) $\mathcal{G}_{wn}[\omega]$, dealing with spatially white Gaussian noise, typically employed for modeling sensor noise, or Directivity Factor (DF) $\mathcal{G}_{dn}[\omega]$, dealing with diffuse noise [18]. WNG and DF are defined as [11]

$$\mathcal{G}_{wn}[\omega] = \frac{|\mathbf{h}^H(\omega)\mathbf{d}(\omega, 0)|^2}{\mathbf{h}^H(\omega)\mathbf{h}(\omega)} , \quad \mathcal{G}_{dn}[\omega] = \frac{|\mathbf{h}^H(\omega)\mathbf{d}(\omega, 0)|^2}{\mathbf{h}^H(\omega)\mathbf{\Gamma}_{dn}(\omega)\mathbf{h}(\omega)}$$
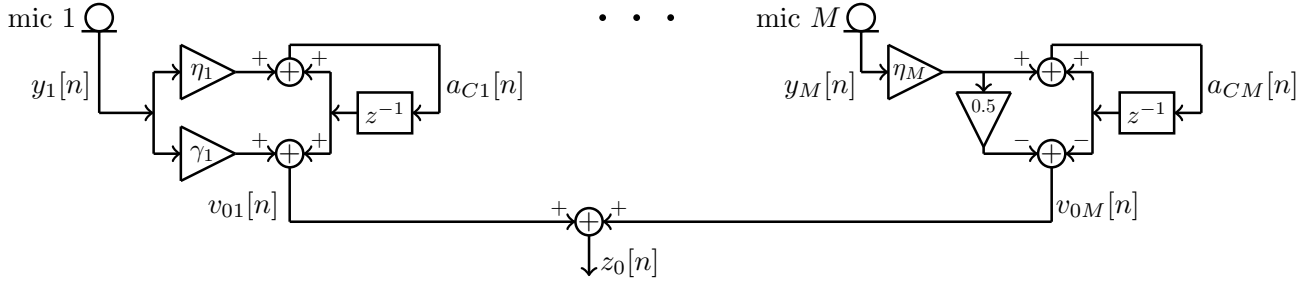
Fig. 3. Detailed signal-flow of the FODMA beamformer implementation based on WDFs.

(a) White Noise Gain for $M = 2$ (b) White Noise Gain for $M = 4$ (c) Directivity Factor for $M = 4$
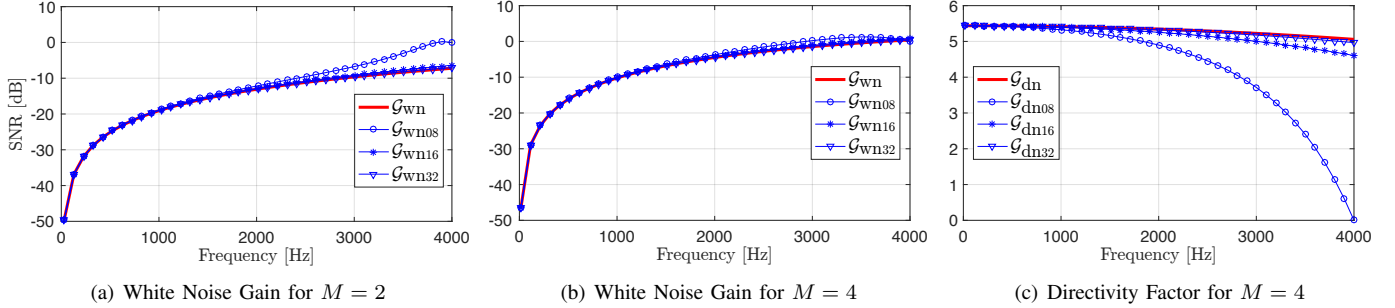
Fig. 4. Comparison between SNRs of continuous-time robust FODMA models computed as in [11] and the corresponding SNRs defined for the discrete-time WDF-based FODMA model with $F_s = 8$ kHz, $F_s = 16$ kHz and $F_s = 32$ kHz. Cases with $M = 2$ and $M = 4$ are plotted. The following parameters are fixed: $\delta = 0.5$ cm and $q = 0.586$ (i.e. the case of the supercardioid is considered, as in [11]).

where the entry at row k and column l of matrix $\mathbf{\Gamma}_{\mathrm{dn}}$ is computed as $[\mathbf{\Gamma}_{\mathrm{dn}}(\omega)]_{kl} = \mathrm{sinc}\,[\omega\,(l - k)\,\tau_0]$ [18].

In the discrete-time WDF model described in Section III continuous-time frequencies are "warped" by the bilinear transform. In the light of this, we will define the DF of a FODMA based on WDF with, for instance, $F_s = 8$ kHz as

$$\mathcal{G}_{dn08}\,[\omega_d] = \frac{|\mathbf{h}^H(\omega)\mathbf{d}(\omega_d, 0)|^2}{\mathbf{h}^H(\omega)\mathbf{\Gamma}_{\mathrm{dn}}(\omega_d)\mathbf{h}(\omega)} \qquad (11)$$

where ω_d is the discrete-time frequency and ω is the continuous-time frequency, being $\omega = 2F_s\tan(\omega_d/(2F_s))$. The WNG $\mathcal{G}_{wn08}\,[\omega_d]$ for $F_s = 8$ kHz is defined similarly; the same holds for $\mathcal{G}_{wn16}$, $\mathcal{G}_{dn16}$ and $\mathcal{G}_{wn32}$, $\mathcal{G}_{dn32}$ which are the WNG and DF relative to $F_s = 16$ kHz and $F_s = 32$ kHz respectively. Fig. 4 shows how the difference between WNG in the continuous-time case and WNG in the discrete-time case is reduced as F_s is increased, both for $M = 2$ and for $M = 4$. Similar considerations hold for the DF. In general, it is worth noticing that for $F_s = 8$ kHz the difference between the continuous-time case and the discrete-time case is small up to about 2 kHz; while for $F_s = 16$ kHz and $F_s = 32$ kHz such difference becomes practically negligible up to at least 4 kHz. Fig. 5 shows the frequency-independent polar patterns of a supercardioid and a dipole, along with the corresponding continuous-time and discrete-time ($F_s = 8$ kHz) frequency-dependent beampatterns evaluated at 1 kHz. Similar results have been obtained for FODMAs with different beampatterns, e.g. hypercardioids or cardioids.

V. CONCLUSIONS AND FUTURE WORK

In this letter a time-domain implementation of FODMA based on WDFs more efficient than those presented in the

(a) Supercardioid   (b) Dipole
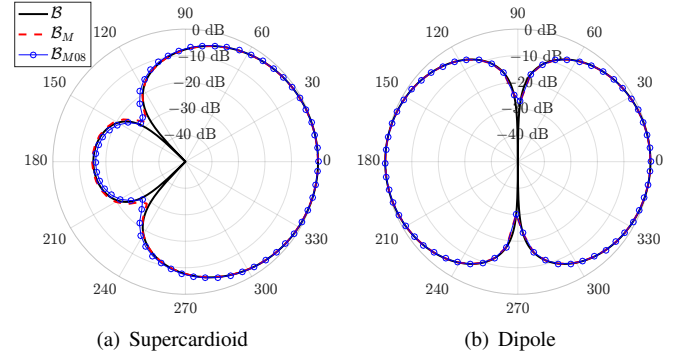
Fig. 5. FODMAs with $q = 0.586$ in Fig. 5(a) (supercardioid) and $q = 1$ in Fig. 5(b) (dipole): frequency-independent beampatterns $\mathcal{B}$ (solid line), frequency-dependent continuous-time beampatterns as in [11], $\mathcal{B}_M(\omega, \theta) = \sum_{m=1}^{M} H_m(\omega)\,[1 + j\,(m - 1)\,\omega\tau_0\cos\theta]$, (dashed line) and frequency-dependent discrete-time beampatterns obtained by the proposed WDF model with $F_s = 8$ kHz, $\mathcal{B}_{M08}(\omega_d, \theta) = \sum_{m=1}^{M} H_m(2F_s\tan(\omega_d/(2F_s)))\,[1 + j\,(m - 1)\,\omega_d\tau_0\cos\theta]$ (line with circles). Frequency-dependent beampatterns are evaluated at 1 kHz with $M = 4$ and $\delta = 0.5$ cm.

literature has been proposed. Moreover, an accuracy study, based on the analysis of WNG and DF, has been presented. Future work will be devoted to the application of the proposed WDF approach to higher order DMAs; moreover, the use of nonlinear WDFs [15], [19]–[26], WDF with active junctions [27], [28] and biparametric WDFs [29] for the design of arbitrary order DMAs will be explored.

REFERENCES

[1] J. Benesty and J. Chen, *Study and Design of Differential Microphone Arrays*, 1st ed., Springer, Ed., 2013.

[2] H. Zhang, J. Chen, and J. Benesty, "Study of nonuniform linear differential microphone arrays with the minimum-norm filter," *Applied Acoustics, Elsevier*, vol. 98, pp. 62–69, Nov 2015.

[3] J. Benesty, J. Chen, and I. Cohen, *Design of Circular Differential Microphone Arrays*, 1st ed., Springer, Ed., 2015.

[4] A. Bernardini, M. D'Aria, R. Sannino, and A. Sarti, "Efficient continuous beam steering for planar arrays of differential microphones," *IEEE Signal Processing Letters*, vol. 24, no. 6, pp. 794–798, June 2017.

[5] G. W. Elko, F. Pardo, D. Lopez, D. Bishop, and P. Gammel, "Surface-micromachined mems microphone," in *Proc. 115th Audio Eng. Society (AES) Convention*, Oct. 2003, pp. 1–8.

[6] G. W. Elko, "Microphone array systems for hands-free telecommunication," *Speech Communications, Elsevier*, vol. 20, no. 3–4, pp. 229–240, Dec. 1996.

[7] M. Buck and M. Rodler, "First order differential microphone arrays for automotive applications," in *Proc. IWAENC*, Sep. 2001, pp. 19–22.

[8] H. Teutsch and G. W. Elko, "First- and second- order adaptive differential microphone arrays," in *Proc. IWAENC*, Sep. 2001, pp. 35–38.

[9] G. W. Elko, "Differential microphone arrays," in *Audio Signal Processing for Next-Generation Multimedia Communication Systems, Y. Huang and J. Benesty*, Eds. Norwell, MA: Kluwer, 2004.

[10] E. De Sena, H. Hacihabiboglu, and Z. Cvetkovic, "On the design and implementation of higher order differential microphones," *IEEE Transactions on Audio, Speech, and Language Processing*, vol. 20, no. 1, pp. 162–174, January 2012.

[11] L. Zhao, J. Benesty, and J. Chen, "Design of robust differential microphone arrays," *IEEE/ACM Transactions on Audio, Speech, and Language Processing*, vol. 22, no. 10, pp. 1455–1466, Oct. 2014.

[12] L. Zhao, J. Benesty, and J. Chen, "Design of robust differential microphone arrays with the Jacobi - Anger expansion," *Applied Acoustics*, vol. 110, pp. 194 – 206, 2016.

[13] Y. Buchris, I. Cohen, and J. Benesty, "First-order differential microphone arrays from a time-domain broadband perspective," in *2016 IEEE International Workshop on Acoustic Signal Enhancement (IWAENC)*, Sept 2016, pp. 1–5.

[14] A. Fettweis, "Wave digital filters: Theory and practice," *Proc. of the IEEE*, vol. 74, pp. 270–327, Feb. 1986.

[15] A. Sarti and G. De Sanctis, "Systematic methods for the implementation of nonlinear wave-digital structures," *IEEE Transactions on Circuits and Systems I: Regular Papers*, vol. 56, pp. 460–472, Feb. 2009.

[16] A. Sarti and G. D. Sanctis, "Memory extraction from dynamic scattering junctions in wave digital structures," *IEEE Signal Processing Letters*, vol. 13, no. 12, pp. 729–732, Dec 2006.

[17] A. Fettweis, "Pseudopassivity, sensitivity, and stability of wave digital filters," *IEEE Trans. Circuit Theory*, vol. 19, pp. 668–673, Nov. 1972.

[18] R. K. Cook, R. V. Waterhouse, R. D. Berendt, S. Edelman, and M. C. Thompson, "Measurement of correlation coefficients in reverberant sound fields," *The Journal of the Acoustical Society of America*, vol. 27, no. 6, pp. 1072–1077, 1955.

[19] K. Meerkötter and R. Scholz, "Digital simulation of nonlinear circuits by wave digital filter principles," in *IEEE Int. Symp. Circuits Syst.*, vol. 1, June 1989, pp. 720–723.

[20] A. Bernardini, K. J. Werner, A. Sarti, and J. O. Smith, "Modeling nonlinear wave digital elements using the Lambert function," *IEEE Transactions on Circuits and Systems I: Regular Papers*, vol. 63, pp. 1231–1242, Aug. 2016.

[21] K. J. Werner, V. Nangia, A. Bernardini, J. O. Smith, and A. Sarti, "An improved and generalized diode clipper model for wave digital filters," in *Proc. 139th Audio Eng. Society (AES) Conv.*, New York, NY, Oct. 29 – Nov. 1 2015.

[22] A. Bernardini, K. J. Werner, A. Sarti, and J. O. Smith, "Multi-port nonlinearities in wave digital structures," in *Proc. 2015 IEEE Int. Symp. Signals Circuits Syst. (ISSCS)*, Iasi, Romania, July 9–10 2015.

[23] A. Bernardini, K. J. Werner, A. Sarti, and J. O. Smith, "Modeling a class of multi-port nonlinearities in wave digital structures," in *Proc. 2015 23rd European Signal Processing Conference (EUSIPCO)*, Nice, France, Aug. 31 – Sept. 4 2015, pp. 669–673.

[24] A. Bernardini and A. Sarti, "Canonical piecewise-linear representation of curves in the wave digital domain," in *Proc. 2017 25th European Signal Processing Conference (EUSIPCO)*, Kos, Greece, Aug. 28 – Sept. 2 2017, pp. 1125–1129.

[25] A. Bernardini and A. Sarti, "Dynamic adaptation of instantaneous nonlinear bipoles in wave digital networks," in *Proc. 2016 24th European Signal Processing Conference (EUSIPCO)*, Budapest, Hungary, Aug. 29 – Sept. 2 2016, pp. 1038–1042.

[26] A. Bernardini, P. Maffezzoni, L. Daniel, and A. Sarti, "Wave-based analysis of large nonlinear photovoltaic arrays," *IEEE Transactions on Circuits and Systems I: Regular Papers*, vol. PP, no. 99, pp. 1–14, 2017.

[27] K. J. Werner, W. R. Dunkel, M. Rest, M. J. Olsen, and J. O. Smith, "Wave digital filter modeling of circuits with operational amplifiers," in *2016 24th European Signal Processing Conference (EUSIPCO)*, Aug. 2016, pp. 1033–1037.

[28] M. Verasani, A. Bernardini, and A. Sarti, "Modeling sallen-key audio filters in the wave digital domain," in *2017 IEEE International Conference on Acoustics, Speech and Signal Processing (ICASSP)*, March 2017, pp. 431–435.

[29] A. Bernardini and A. Sarti, "Biparametric wave digital filters," *IEEE Transactions on Circuits and Systems I: Regular Papers*, vol. 64, no. 7, pp. 1826–1838, July 2017.